5-27-2011

Principal angles and principal azimuths of frustrated total internal reflection and optical tunneling by an embedded low-index thin film

R. M.A. Azzam
University of New Orleans, razzam@uno.edu

F. F. Sudradjat

Principal angles and principal azimuths of frustrated total internal reflection and optical tunneling by an embedded low-index thin film

R. M. A. Azzam[1,*] and F. F. Sudradjat[2,3]

[1]*Department of Electrical Engineering, University of New Orleans, New Orleans, Louisiana 70148, USA*
[2]*Department of Electrical and Computer Engineering, Boston University, Boston, Massachusetts 02215, USA*
[3]*ffsudrad@bu.edu*
**Corresponding author: razzam@uno.edu*

Received March 16, 2011; accepted April 13, 2011;
posted April 22, 2011 (Doc. ID 144296); published May 27, 2011

The condition for obtaining a differential (or ellipsometric) quarter-wave retardation when p- and s-polarized light of wavelength λ experience frustrated total internal reflection (FTIR) and optical tunneling at angles of incidence $\phi \geq$ the critical angle by a transparent thin film (medium 1) of low refractive index n_1 and uniform thickness d, which is embedded in a transparent bulk medium 0 of high refractive index n_0 takes the simple form: $-\tanh^2 x = \tan\delta_p \tan\delta_s$, in which $x = 2\pi n_1(d/\lambda)(N^2\sin^2\phi - 1)^{1/2}$, $N = n_0/n_1$, and δ_p, δ_s are 01 interface Fresnel reflection phase shifts for the p and s polarizations. From this condition, the ranges of the principal angle and normalized film thickness d/λ are obtained explicitly. At a given principal angle, the associated principal azimuths ψ_r, ψ_t in reflection and transmission are determined by $\tan^2\psi_r = -\sin 2\delta_s/\sin 2\delta_p$ and $\tan^2\psi_t = -\tan\delta_p/\tan\delta_s$, respectively. At a unique principal angle ϕ_e given by $\sin^2\phi_e = 2/(N^2+1)$, $\psi_r = \psi_t = 45°$ and linear-to-circular polarization conversion is achieved upon FTIR and optical tunneling simultaneously. The intensity transmittances of p- and s-polarized light at any principal angle are given by $\tau_p = \tan\delta_p/\tan(\delta_p - \delta_s)$ and $\tau_s = -\tan\delta_s/\tan(\delta_p - \delta_s)$, respectively. The efficiency of linear-to-circular polarization conversion in optical tunneling is maximum at ϕ_e. © 2011 Optical Society of America

OCIS codes: 240.0310, 240.7040, 260.2130, 260.5430, 260.6970, 310.6860.

1. INTRODUCTION

At a dielectric–conductor planar interface, a principal angle is defined as an angle of incidence at which incident linearly polarized monochromatic light of the proper azimuth, called the principal azimuth, is reflected circularly polarized [1–3]. Depending on the value of the relative complex dielectric function of the two media, one, two, or three principal angle–principal azimuth pairs may exist [2,3]. For light reflection by a transparent thin film on an absorbing substrate, there is a continuum of principal angles and an associated range of principal azimuths [4].

A previous paper [5] presented a detailed analysis of the phase shifts that monochromatic p- and s-polarized light of wavelength λ experience in frustrated total internal reflection (FTIR) and optical tunneling at angles of incidence $\phi \geq$ the critical angle by a thin film of low refractive index n_1 and uniform thickness d, which is embedded in a transparent bulk medium of high refractive index n_0 (typically a uniform air gap, $n_1 = 1$, between parallel plane faces of two transparent prisms; Fig. 1). In a related paper [6], Azzam and Spinu described an FTIR, 2–12 μm wavelength-tunable circular-polarization beam splitter that uses a variable-thickness air gap between two Ge prisms.

In this paper, closed-form solutions for the principal angles, principal azimuths, and film thicknesses that produce linear-to-circular polarization conversion in FTIR and optical tunneling by an embedded low-index thin film are obtained. The principal angle condition is considered analytically and graphically in Section 2. At a given principal angle ϕ and given refractive index ratio $N = n_0/n_1$, an explicit solution for the normalized film thickness d/λ that produces dual quarter-wave retardation (QWR) in reflection and transmission is derived in Section 3. In Section 4, the associated principal azimuths of reflection and transmission are obtained in terms of the 01 interface Fresnel reflection phase shifts for the p and s polarizations. Section 5 is devoted to the special case of dual circular polarization in reflection and transmission at the unique incidence angle of equal tunneling of the p and s polarizations. In Section 6, the intensity reflectances and transmittances of p- and s-polarized light in FTIR and optical tunneling are obtained as functions of the principal angle ϕ and refractive index ratio N. Section 7 gives a brief summary of the paper. In Appendix A, alternate expressions of the principal azimuths of reflection and transmission are presented, and, in Appendix B, the condition of maximum linear-to-circular polarization conversion in optical tunneling is considered.

2. PRINCIPAL ANGLES OF FTIR AND OPTICAL TUNNELING

The changes of polarization that accompany FTIR and optical tunneling are determined by the ratios of complex-amplitude reflection (R) and transmission (T) coefficients of p- and s-polarized light that account for coherent multiple-plane-wave interference within the embedded layer. These ellipsometric functions [7] are expressed as

$$\rho_r = R_p/R_s = \tan\psi_r \exp(j\Delta_r),$$
$$\rho_t = T_p/T_s = \tan\psi_t \exp(j\Delta_t). \quad (1)$$

1084-7529/11/061256-06$15.00/0

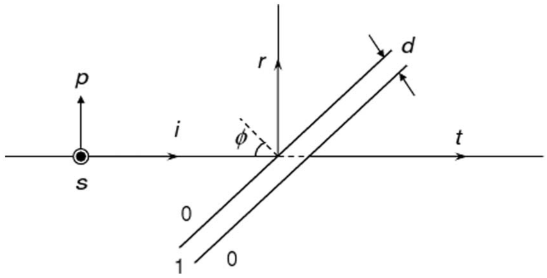

Fig. 1. Reflection and transmission of p- and s-polarized light at an angle of incidence ϕ by a uniform layer of thickness d and refractive index n_1 (medium 1), which is embedded in a bulk medium 0 of refractive index n_0.

In [5], it is shown that

$$\Delta_r = \Delta_t, \tag{2}$$

$$\tan\psi_r/\tan\psi_t = \sin\delta_s/\sin\delta_p = (N^2+1)\sin^2\phi - 1. \tag{3}$$

In Eq. (3), $N = n_0/n_1$ is the high-to-low index ratio and δ_p, δ_s are 01 interface Fresnel reflection phase shifts for the p and s polarizations. Starting from results already obtained in [5], ρ_r is written as

$$\rho_r = \frac{\tanh x \cos\delta_s - j\sin\delta_s}{\tanh x\cos\delta_p - j\sin\delta_p}, \tag{4}$$

$$x = 2\pi n_1 (d/\lambda)(N^2\sin^2\phi - 1)^{1/2}. \tag{5}$$

At a principal angle,

$$\mathrm{Re}\rho_r = 0, \tag{6}$$

and substitution of ρ_r from Eq. (4) in Eq. (6) leads to

$$\tanh^2 x\cos\delta_p\cos\delta_s + \sin\delta_p\sin\delta_s = 0, \tag{7}$$

$$-\tanh^2 x = \tan\delta_p\tan\delta_s. \tag{8}$$

Equation (8) is the simplest possible form of the principal-angle condition in FTIR by an embedded low-index thin film. (This result is also obtained by setting the denominator of the right-hand side of Eq. (13) in [5] equal to zero.) For specified values of n_1, N, Eq. (8) represents the constraint on d/λ, ϕ such that the overall differential reflection and transmission phase shifts are quarter-wave, i.e., $\Delta_r = \Delta_t = \pi/2$.

From the known expressions of the 01 interface Fresnel reflection phase shifts δ_ν ($\nu = p, s$) [8], the right-hand side of Eq. (8) can be cast as a function of ϕ of the form

$$\tan\delta_p\tan\delta_s = \left(\frac{\sin^2\phi_p}{\sin^2\phi_s}\right)\frac{(\sin^2\phi - \sin^2\phi_c)(1-\sin^2\phi)}{(\sin^2\phi - \sin^2\phi_p)(\sin^2\phi - \sin^2\phi_s)}. \tag{9}$$

In Eq. (9), $\phi_c = \sin^{-1}(1/N)$ is the critical angle and ϕ_p, ϕ_s are the angles of incidence at which $\delta_p = \pi/2$ and $\delta_s = \pi/2$, respectively [8].

As an example, consider a uniform air gap ($n_1 = 1$) between two Ge prisms ($N = 4$) in the IR. Figure 2 shows the product of tangents given by Eq. (9) as a function of ϕ for $\phi_c \le \phi \le 90°$ as a continuous line. Singularities of this function appear at $\phi_p = 14.90°$ and $\phi_s = 46.79°$ as expected. In Fig. 2, a family of curves (dashed curves) that represent the left-hand side of Eq. (8) is also plotted versus ϕ for discrete values of $d/\lambda = 0.005$, 0.02 to 0.20 in equal steps of 0.02, and 10. Solutions of Eq. (8) correspond to points of intersection of the negative branch of the product-of-tangents function ($\phi_p < \phi < \phi_s$) and the dashed lines that represent $-\tanh^2 x$ (e.g., points A and B for $d/\lambda = 0.08$). Principal angles of the Ge–air–Ge system cease to exist for very thin films with $d/\lambda < 0.059$. At large film thicknesses (e.g., $d/\lambda \ge 10$), optical tunneling is negligible and TIR at the 01 interface is restored. In this large-thickness limit, $\tanh^2 x = 1$ and Eq. (8) reduces to

$$\tan\delta_p\tan\delta_s = -1. \tag{10}$$

Equation (10) indicates that $\delta_p - \delta_s = \pi/2$, which is the principal-angle condition of TIR at the 01 interface. The full range of principal angles $\phi_1 \le \phi \le \phi_2$ is defined in Fig. 2 by the points of intersection P_1 and P_2 at which Eq. (10) is satisfied. The corresponding limiting angles ϕ_1 and ϕ_2 are given by [8]

$$\sin^2\phi_{1,2} = [(N^2+1)\mp(N^4 - 6N^2 + 1)^{1/2}]/4N^2. \tag{11}$$

Acceptable solutions of Eq. (11) exist if

$$N \ge \sqrt{2} + 1 = 2.414. \tag{12}$$

For the Ge–air interface $N = 4$, $\phi_1 = 15.04°$ (which is slightly above the critical angle $\phi_c = 14.48°$) and $\phi_2 = 42.93°$.

3. FILM THICKNESS FOR QWR AT A GIVEN PRINCIPAL ANGLE

For an index ratio $N > 2.414$ and a principal angle ϕ in the range $\phi_1 \le \phi \le \phi_2$ defined by Eq. (11), the value of $\tanh x$ that satisfies the principal-angle condition is determined by Eqs. (8) and (9). From $\tanh x$,

$$X = \exp(-2x) = (1 - \tanh x)/(1 + \tanh x) \tag{13}$$

is calculated. Next, the normalized film thickness that produces QWR in reflection and transmission ($\Delta_r = \Delta_t = \pi/2$) is obtained from Eqs. (5) and (13) as

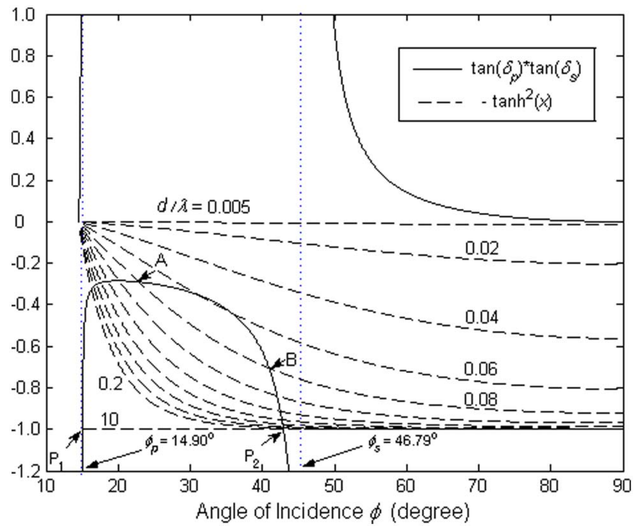

Fig. 2. (Color online) Graphical construction that illustrates the range of possible solutions of Eq. (8).

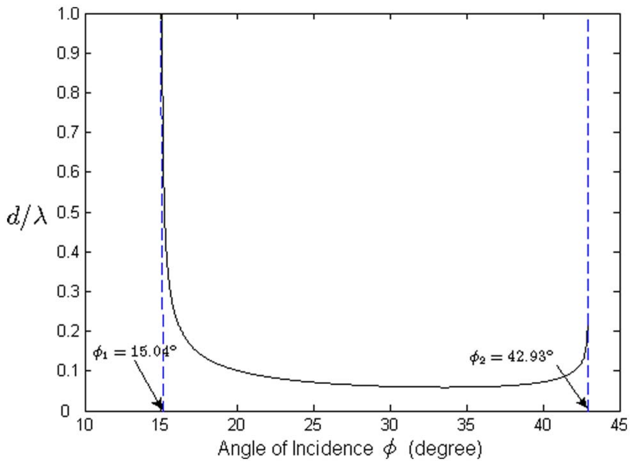

Fig. 3. (Color online) Normalized thickness d/λ of a uniform air gap between two IR-transparent Ge prisms ($n_1 = 1, N = 4$) that produces $\Delta_r = \Delta_t = \pi/2$ is plotted as a function of principal angle ϕ over the full range from $\phi_1 = 15.04°$ to $\phi_2 = 42.93°$.

$$d/\lambda = -(\ln X)/[4\pi n_1 (N^2 \sin^2\phi - 1)^{1/2}]. \quad (14)$$

As an example, the above algorithm is applied to a uniform air gap between two IR-transparent Ge prisms ($n_1 = 1, N = 4$) at $\phi = 30°$; this gives $\delta_p = 165.75°$, $\delta_s = 53.13°$, $\tanh x = (-\tan\delta_p \tan\delta_s)^{1/2} = 0.581914$, $X = 0.264291$, and $d/\lambda = 0.061138$.

Use of the same algorithm for the Ge–air–Ge system over the full range of principal angles from $\phi_1 = 15.04°$ to $\phi_2 = 42.93°$, d/λ at which $\Delta_r = \Delta_t = \pi/2$ is obtained as a function of principal angle ϕ, as shown in Fig. 3. Except for a change of scale of the ordinate axis, this graph is the same as the one obtained by Azzam and Spinu (Fig. 2 in [6]) using an iterative numerical technique.

4. REFLECTION AND TRANSMISSION PRINCIPAL AZIMUTHS AT A GIVEN PRINCIPAL ANGLE

At a principal angle, $\cos\Delta_r = 0$, $\sin\Delta_r = 1$, $\mathrm{Re}\rho_r = 0$ [Eq. (6)], and ρ_r reduce to

$$\rho_r = j\tan\psi_r. \quad (15)$$

In Eq. (15), ψ_r is the associated principal azimuth (the angle between the electric-field vector of incident linearly polarized light and the plane of incidence) that produces circularly polarized reflected light. From Eqs. (4) and (15), we obtain

$$\mathrm{Im}\rho_r = \tan\psi_r = \frac{\tanh^2 x \sin(\delta_p - \delta_s)}{\tanh^2 x \cos^2\delta_p + \sin^2\delta_p}. \quad (16)$$

Substitution of $\tanh^2 x = -\tan\delta_p \tan\delta_s$ [Eq. (8)] in Eq. (16) and use of trigonometric identities lead to an explicit expression for the principal azimuth ψ_r in terms of the 01 interface TIR phase shifts δ_ν ($\nu = p, s$):

$$\tan^2\psi_r = -\sin 2\delta_s / \sin 2\delta_p. \quad (17)$$

At the same principal angle, the principal azimuth ψ_t that produces circular polarization of the transmitted (instead of reflected) light is derived from Eqs. (3) and (17) as

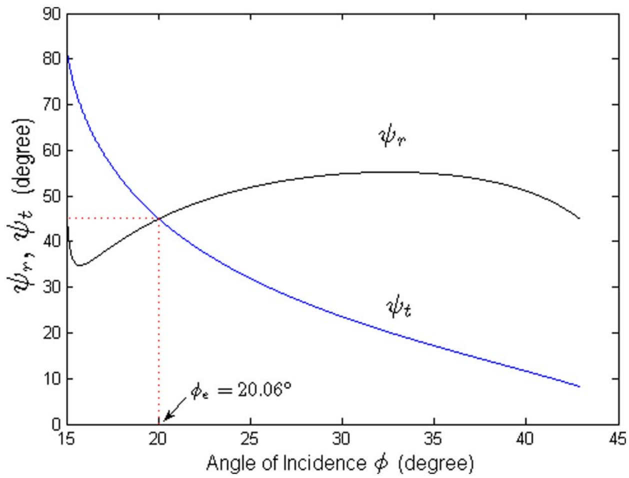

Fig. 4. (Color online) Reflection and transmission principal azimuths ψ_r, ψ_t [Eqs. (17) and (18)] are plotted as functions of the principal angle ϕ for a uniform air gap between two IR-transparent Ge prisms ($n_1 = 1, N = 4$) over the full range of principle angles $\phi_1 \le \phi \le \phi_2$.

$$\tan^2\psi_t = -\tan\delta_p / \tan\delta_s. \quad (18)$$

An air gap between two Ge prisms ($n_1 = 1$, $N = 4$) with thickness $d/\lambda = 0.061138$ has a principal angle $\phi = 30°$ (Section 3). Substitution of $\delta_p = 165.75°$ at $\delta_s = 53.13°$, $\phi = 30°$ in Eqs. (17) and (18) gives $\psi_r = 54.816°$, $\psi_t = 23.578°$. Calculation of ψ_r, ψ_t as functions of ϕ over the full range of principle angles $\phi_1 \le \phi \le \phi_2$ of the Ge–air–Ge system produces the two curves shown in Fig. 4.

In Appendix A, we give alternate explicit expressions of ψ_r, ψ_t as functions of ϕ for a given N and locate the angular positions of the minimum and maximum of the ψ_r-versus-ϕ curve.

5. DUAL CIRCULAR POLARIZATION OF REFLECTED AND TRANSMITTED LIGHT AT ONE PRINCIPAL ANGLE

From Eq. (3), the principal azimuths of FTIR and optical tunneling are equal, $\psi_r = \psi_t$, at one principal angle ϕ_e, given by

$$\sin^2\phi_e = 2/(N^2 + 1). \quad (19)$$

ϕ_e of Eq. (19) is the incidence angle of equal tunneling of p- and s-polarized light [9,10] so that $\psi_r = \psi_t = 45°$. In Fig. 4, for $N = 4$, $\psi_r = \psi_t = 45°$ at $\phi_e = \sin^{-1}(2/17)^{1/2} = 20.06°$.

It is worthwhile to recall that ϕ_e is the angle of incidence at which phase difference $(\delta_p - \delta_s)$ is maximum and the average phase shift is $(\delta_p + \delta_s)/2 = \pi/2$ [8].

Also, at ϕ_e, the Fresnel reflection phase shifts at the 01 interface [8] simplify to

$$\tan(\delta_s/2) = 1/N, \qquad \tan(\delta_p/2) = N. \quad (20)$$

Equation (20) indicates that δ_s and δ_p at ϕ_e are equal to double the Brewster angles of internal and external reflection at the 01 interface, respectively.

Still another curious property of ϕ_e is that, for a given N, the product of tangents given by Eq. (9) reaches a maximum at that angle. This can be proved by substituting $\sin^2\phi = u$ in Eq. (9) and setting the derivative of the right-hand side with respect to u equal to zero. By use of Eq. (20) and the trigonometric identity $\tan x = 2\tan(x/2)/[1 - \tan^2(x/2)]$, the maximum value of $\tan\delta_p \tan\delta_s$ at ϕ_e is obtained:

$$(\tan\delta_p \tan\delta_s)_{\max} = -4N^2/(N^2-1)^2. \quad (21)$$

At ϕ_e, Eqs. (8), (13), and (21) lead to

$$\tanh x = 2N/(N^2-1), \quad (22)$$

$$X = (N^2-2N-1)/(N^2+2N-1). \quad (23)$$

The value of d/λ that produces dual QWR with equal throughput for the p and s polarizations in FTIR and optical tunneling at ϕ_e is obtained by substituting X from Eq. (23) and $(N^2\sin^2\phi_e-1)^{1/2} = [(N^2-1)/(N^2+1)]^{1/2}$ in Eq. (14); this gives

$$d/\lambda = (4\pi n_1)^{-1}\left(\frac{N^2+1}{N^2-1}\right)^{1/2}\ln\left(\frac{N^2+2N-1}{N^2-2N-1}\right). \quad (24)$$

For the Ge–air–Ge system ($n_1 = 1, N = 4$), $\phi_e = 20.06°$ and the normalized air-gap thickness for dual QWR in reflection and transmission is obtained from Eq. (24):

$$d/\lambda = (4\pi)^{-1}(17/15)^{1/2}\ln(23/7) = 0.100778. \quad (25)$$

The closed-form solution for d/λ [Eq. (24)] supersedes any iterative numerical approach [6]. Figure 5 is a graph of d/λ as a function of N calculated form Eq. (24) over the range $2.5 \le N \le 6.0$.

6. REFLECTANCES AND TRANSMITTANCES OF *p*- AND *s*- POLARIZED LIGHT AT A GIVEN PRINCIPAL ANGLE

The intensity reflectances and transmittances of p- and s-polarized light are obtained by taking the squared absolute value of the corresponding complex-amplitude reflection and transmission coefficients $R_p, R_s; T_p, T_s$ given in [5]. The resulting expressions are functions of the film thickness parameter x [Eq. (5)] and the 01 interface Fresnel reflection phase shifts δ_ν $(\nu = p, s)$:

$$\mathsf{R}_\nu = |R_\nu|^2 = \frac{\cosh 2x - 1}{\cosh 2x - \cos 2\delta_\nu}, \qquad \nu = p, s; \quad (26)$$

$$\tau_\nu = 1 - |R_\nu|^2 = \frac{1-\cos 2\delta_\nu}{\cosh 2x - \cos 2\delta_\nu}, \qquad \nu = p, s. \quad (27)$$

From Eq. (27), the principal-angle condition of Eq. (8), and the identity

$$\cosh 2x = (1+\tanh^2 x)/(1-\tanh^2 x), \quad (28)$$

the following expressions of the p and s intensity transmittances are obtained:

$$\tau_p = \tan\delta_p/\tan(\delta_p-\delta_s), \qquad \tau_s = -\tan\delta_s/\tan(\delta_p-\delta_s). \quad (29)$$

Note that, from Eq. (29), $\tau_p/\tau_s = \tan^2\psi_t = -\tan\delta_p/\tan\delta_s$ in agreement with Eq. (18). The corresponding intensity reflectances are given by

$$\mathsf{R}_\nu = 1 - \tau_\nu \quad \nu = p, s. \quad (30)$$

Substitution of δ_p, δ_s $(\delta_p-\delta_s)$ as functions of N and ϕ from [8] in Eqs. (29) yields

$$\tau_p = \frac{2N^2\sin^4\phi - (N^2+1)\sin^2\phi + 1}{-(N^4+1)\sin^4\phi + (N^2+1)\sin^2\phi}, \quad (31)$$

$$\tau_s = \frac{2N^2\sin^4\phi - (N^2+1)\sin^2\phi + 1}{2N^2\sin^4\phi - (N^2+1)\sin^2\phi}. \quad (32)$$

Equations (31) and (32) are valid over the full range of principal angles $\phi_1 \le \phi \le \phi_2$ defined by Eq. (11) and give exact mathematical representation of the families of curves presented in Fig. 5 in [6]. Both transmittances are zero at the limiting angles ϕ_1 and ϕ_2 given by Eq. (11) as can be verified by setting the common numerator of Eqs. (31) and (32) equal to zero.

For a given N, the transmittance $\tau_p(\phi)$ of Eq. (31) reaches a maximum at a principal angle of incidence given by

$$\sin^2\phi_{p\max} = (N^2+1)/(N^2-1)^2. \quad (33)$$

Likewise, for a given N, the transmittance $\tau_s(\phi)$ of Eq. (32) reaches a maximum at a principal angle of incidence given by

$$\sin^2\phi_{s\max} = (N^2+1)/4N^2. \quad (34)$$

Equations (33) and (34) are obtained by substituting $\sin^2\phi = u$ in Eqs. (31) and (32) and setting the derivative of the right-hand side of each equation with respect to u equal to zero.

For a given N, the maximum transmittances at $\phi_{p\max}$ and $\phi_{s\max}$ are equal,

$$\tau_{p\max} = \tau_{s\max} = \frac{N^4-6N^2+1}{N^4+2N^2+1}, \quad (35)$$

and the corresponding principal azimuths are related by

$$\psi_t(\phi_{s\max}) = 90° - \psi_t(\phi_{p\max}), \quad (36)$$

$$\psi_t(\phi_{p\max}) = \arctan\left[\frac{N^6-3N^4-3N^2+1}{2N^2(N^2+1)}\right]^{1/2}. \quad (37)$$

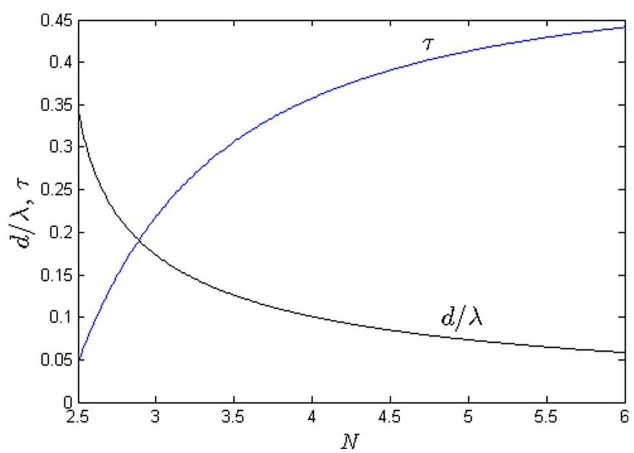

Fig. 5. (Color online) Normalized thickness d/λ of a low-index embedded layer that produces circular polarization in FTIR and optical tunneling at ϕ_e and $\psi_r = \psi_t = 45°$ [Eq. (24)] is plotted as a function of the refractive index ratio N over the range $2.5 \le N \le 6.0$. Equal transmittance of p- and s-polarized light $\tau_p(\phi_e) = \tau_s(\phi_e) = \tau$ [Eq. (39)] is also shown as a function of N.

For the Ge–air–Ge system in the IR, $N = 4$ and Eqs. (33)–(37) give

$$\phi_{p\,\max} = 15.95°, \qquad \phi_{s\,\max} = 31.02°;$$
$$\tau_{p\,\max} = \tau_{s\,\max} = 0.5571; \qquad \psi_t(\phi_{p\,\max}) = 67.84°,$$
$$\psi_t(\phi_{s\,\max}) = 22.16°. \tag{38}$$

The analytical expressions presented here fully explain the results previously obtained by Azzam and Spinu using a numerical technique (see Fig. 5 in [6]).

When the denominators of the right-hand sides of Eqs. (31) and (32) are equal, the p and s transmittances become equal, and the condition of equal tunneling of the p and s polarizations [Eq. (19)] at $\phi = \phi_e$ is recovered. At ϕ_e, the equal throughputs for the p and s polarizations are given by

$$\tau_p(\phi_e) = \tau_s(\phi_e) = 1 - \frac{1}{2}\left(\frac{N^2+1}{N^2-1}\right)^2. \tag{39}$$

The same transmittance of p- and s-polarized light at $\phi = \phi_e$ $[\tau_p(\phi_e) = \tau_s(\phi_e) = \tau]$ is plotted as a function of N in Fig. 5. For $N = 4$, Eq. (39) gives $\tau_p(\phi_e) = \tau_s(\phi_e) = 0.35778$ in agreement with [6].

Another curious result of this section is that $\phi_{s\,\max}$ given by Eq. (34) is also the angle of incidence at which $\delta_p = 3\delta_s$ [8].

In Appendix B, it is shown that the efficiency of linear-to-circular polarization conversion upon optical tunneling is maximum at $\phi = \phi_e$.

7. CONCLUSION

Highlights of this paper are summarized as follows.

1. The principal-angle condition of FTIR and optical tunneling by an embedded low-index thin film is given in concise form by Eq. (8). For selected refractive indices n_1, N, Eq. (8) represents the constraint on the normalized film thickness and principal angle $(d/\lambda, \phi)$ such that the differential phase shifts in reflection and transmission are quarter-wave. Figure 2 illustrates the domain of $d/\lambda, \phi$ for which acceptable solutions of Eq. (8) exist when $n_1 = 1$, $N = 4$.
2. For given values of n_1, N, d/λ that leads to QWR in reflection and transmission (i.e., $\Delta_r = \Delta_t = \pi/2$) at a principal angle ϕ is explicitly determined by Eq. (14).
3. Equations (17) and (18) determine the reflection and transmission principal azimuths ψ_r, ψ_t in terms of the 01 interface Fresnel reflection phase shifts δ_ν $(\nu = p, s)$.
4. At the angle ϕ_e given by Eq. (19), $\psi_r = \psi_t = 45°$, and circular polarization in FTIR and optical tunneling is achieved simultaneously at thickness-to-wavelength ratio d/λ given by Eq. (24).
5. At a given principal angle, the throughputs for the p and s polarizations in optical tunneling are given by Eqs. (29), (31), and (32). These transmittances have maxima at principal angles given by Eqs. (33) and (34), respectively.
6. The efficiency of linear-to-circular polarization conversion upon optical tunneling is maximum [Eq. (B7)] at $\phi = \phi_e$.

APPENDIX A

By substituting the Fresnel interface reflection phase shifts δ_ν $(\nu = p, s)$ as functions of N, ϕ from [8] in Eqs. (18) and (17), we obtain

$$\tan^2\psi_t = -\left(\frac{u_p}{u_s}\right)\left(\frac{u - u_s}{u - u_p}\right), \tag{A1}$$

$$\tan^2\psi_r = -\left(\frac{4u_p}{u_s u_e^2}\right)\left(\frac{(u - u_s)(u - 0.5u_e)^{1/2}}{(u - u_p)}\right). \tag{A2}$$

In Eq. (A1) and (A2), $u = \sin^2\phi$ and u_p, u_s, u_e are the values of u evaluated at the special angles ϕ_p, ϕ_s, $\phi_e = \phi_a$ defined in [8] that depend on N only. Equations (A1) and (A2) provide explicit expressions for the principal azimuths ψ_r, ψ_t as functions of the principal angle ϕ for any given N. For $N = 4$, the curves of ψ_r, ψ_t versus ϕ are plotted in Fig. 4.

In Fig. 4, it is apparent that ψ_t decreases monotonically as ϕ increases, whereas ψ_r exhibits a minimum and a maximum as a function of ϕ. The angular positions of the minimum and maximum of ψ_r are determined by setting the first derivative of the right-hand side of Eq. (A2) with respect to u equal to zero. This gives a quadratic equation in u whose roots are

$$u_\mp = (1/4)\Big\{(3u_p + u_s) \mp \sqrt{(3u_p + u_s)^2 + 4u_e(u_s - u_p) - 16u_p u_s}\Big\}. \tag{A3}$$

For $N = 4$, $u_p = 17/257$, $u_s = 17/32$, $u_e = 2/17$, and Eq. (A3) gives $u_- = 0.073719$, $\phi_- = 15.7542°$; $u_+ = 0.291128$, $\phi_+ = 32.6539°$, which exactly locate the angular positions of the minimum and maximum of ψ_r in Fig. 4.

APPENDIX B

At a given principal angle-principal azimuth pair (ϕ, ψ_t), incident linearly polarized light of intensity I_i is partially transmitted as circularly polarized with intensity I_t given by

$$I_t = I_i(\tau_p\cos^2\psi_t + \tau_s\sin^2\psi_t). \tag{B1}$$

The efficiency of linear-to-circular polarization conversion in optical tunneling is given by

$$\eta_{\rm LTC} = I_t/I_i = (\tau_p\cos^2\psi_t + \tau_s\sin^2\psi_t). \tag{B2}$$

Given that $\tau_p/\tau_s = \tan^2\psi_t$, Eq. (B2) becomes

$$\eta_{\rm LTC} = I_t/I_i = 2\tau_p\cos^2\psi_t = 2\tau_s\sin^2\psi_t. \tag{B3}$$

Substitution of Eqs. (18) and (29) and the Fresnel interface reflection phase shifts δ_ν $(\nu = p, s)$ as functions of N, ϕ [8] in Eq. (B3) leads to

$$\eta_{\rm LTC} = [u_p/(u_p - u_s)][2 - 2u_s u^{-1} + u_c u^{-2}]. \tag{B4}$$

In Eq. (B4), $u = \sin^2\phi$ and u_c, u_p, u_s are the values of u evaluated at the angles ϕ_c, ϕ_p, ϕ_s defined in [8]. By setting

$$d\eta_{\rm LTC}/du = 0 \tag{B5}$$

in Eq. (B4), the value of u at which $\eta_{\rm LTC}$ is maximum is obtained:

$$u = u_c/u_s = 2/(N^2 + 1). \tag{B6}$$

Equations (19) and (B6) confirm that $\eta_{\rm LTC}$ is maximum at the angle ϕ_e of equal tunneling of the p and s polarizations

($\psi_t = 45°$); the associated maximum value of η_{LTC} is obtained from Eqs. (B3) and (39) as

$$\eta_{\mathrm{LTC}}^{\max} = \tau_p(\phi_e) = \tau_s(\phi_e) 1 - \frac{1}{2}\left(\frac{N^2+1}{N^2-1}\right)^2. \quad \text{(B7)}$$

REFERENCES

1. H. B. Holl, "Specular reflection and characteristics of reflected light," J. Opt. Soc. Am. **57**, 683–690 (1967).
2. R. M. A. Azzam, "Contours of constant principal angle and constant principal azimuth in the complex ε plane," J. Opt. Soc. Am. **71**, 1523–1528 (1981).
3. R. M. A. Azzam and A. Alsamman, "Plurality of principal angles for a given pseudo-Brewster angle when polarized light is reflected at a dielectric-conductor interface," J. Opt. Soc. Am. A **25**, 2858–2864 (2008).
4. R. M. A. Azzam and A.-R. M. Zaghloul,"Principal angle, principal azimuth, and principal-angle ellipsometry of film-substrate systems," J. Opt. Soc. Am. **67**, 1058–1065 (1977).
5. R. M. A. Azzam, "Phase shifts in frustrated total internal reflection and optical tunneling by an embedded low-index thin film," J. Opt. Soc. Am. A **23**, 960–965 (2006).
6. R. M. A. Azzam and C. L. Spinu,"Linear-to-circular polarization transformation upon optical tunneling through an embedded low-index film," Opt. Lett. **30**, 3183–3185 (2005).
7. R. M. A. Azzam and N. M. Bashara, *Ellipsometry and Polarized Light* (North-Holland, 1987).
8. R. M. A. Azzam, "Phase shifts that accompany total internal reflection at a dielectric-dielectric interface," J. Opt. Soc. Am. A **21**, 1559–1563 (2004).
9. P. W. Baumeister, "Optical tunneling and its application to optical filters," Appl. Opt. **6**, 897–905 (1967).
10. R. W. Astheimer, G. Falbel, and S. Minkowitz, "Infrared modulation by means of frustrated total internal reflection," Appl. Opt. **5**, 87–91 (1966).